Original Article
Itaconate targets the ERK2 signal to suppress estrogen receptor-positive breast cancer cell growth

Hsueh-Chun Wang[1], Yi-Chuan Li[2], Mien-Chie Hung[1,3,4,5,6]

[1]Graduate Institute of Biomedical Sciences, China Medical University, Taichung 406040, Taiwan; [2]Department of Biological Science and Technology, China Medical University, Taichung 406040, Taiwan; [3]Institute of Biochemistry and Molecular Biology, China Medical University, Taichung 406040, Taiwan; [4]Research Center for Cancer Biology, China Medical University, Taichung 406040, Taiwan; [5]Cancer Biology and Precision Therapeutics Center, China Medical University, Taichung 406040, Taiwan; [6]Center for Molecular Medicine, China Medical University, Taichung 406040, Taiwan

Abstract: Over 70% of breast cancers are estrogen receptor (ER)-positive, with Tamoxifen (Tam) being a standard treatment. However, around 40% of these cancers develop resistance to Tam, which poses a significant clinical challenge. The ACOD1/itaconate (ITA) axis, a metabolic pathway that produces itaconate, has shown promise in inhibiting the growth of ER-positive breast cancer cells. Nonetheless, it remains unclear how effective ITA is against Tam-resistant breast cancer cells and the underlying mechanisms involved. The current report found that Tam-resistant cells exhibit increased sensitivity to ITA compared to their parental cells and show a synergetic effect in combination treatment with Tam. An unbiased proteomic analysis revealed that upregulating the ERK2 signaling pathway contributes to the sensitivity of ER-positive breast cancer cells to ITA. ITA treatment increases ERK2 phosphorylation at T185/Y187 sites by directly alkylating cysteine 254, leading to ERK2 activation and subsequent cell growth inhibition. These effects were abolished in ITA allylation-resistant cells when a cysteine residue was replaced with serine. Additionally, itaconate-induced ERK2 phosphorylation and activation inhibits the growth of Tam-resistant breast cancer cells, which effect is advanced in phosphorylation-mimic ERK2_T185E-expressing cells but blocked in those expressing non-phosphorylation-mimic ERK2_T185A. Furthermore, activated ERK2 interacts physically with API5 to disrupt API5's localization to the nucleus speckle, where API5 may interact with other molecules critical in regulating cell growth-related genes. Our findings clarify the mechanism through which ITA exerts its effects on tamoxifen-sensitive and resistant breast cancer cells and highlight the potential of itaconate as an alternative treatment strategy against breast cancer.

Keywords: Aconitate decarboxylase 1, breast cancer, estrogen receptor, extracellular signal-regulated kinase 2, itaconate, tamoxifen

Introduction

Over 70% of breast cancers are classified as estrogen receptor (ER)-positive with tamoxifen (Tam) as a standard treatment [1]. However, around 40% of these cancers eventually develop resistance to Tam, raising a significant challenge in treatment [2-6]. Cancer cells often adjust their biochemical pathways to meet increased energy demands, leading to changes in metabolites that are crucial for tumor development and progression [7, 8]. These metabolic alterations, including enhanced aerobic glycolysis, reduced oxidative phosphorylation, and an increased generation of biosynthetic intermediates, are necessary for cancer cell growth, proliferation, and drug resistance [9].

Itaconate (ITA) is a metabolite synthesized from the conversion of cis-aconitate by the aconitate decarboxylase 1 (ACOD1) in the tricarboxylic acid (TCA) cycle. Itaconate production disrupts the TCA cycle and inhibits succinate dehydrogenase (SDH), which alters oxidative phosphorylation and affects where the cells get their energy from [10-12]. Several studies have demonstrated that ITA and its derivatives, such as 4-octyl-itaconate (4-OI),

can modify cysteine residues in proteins via a process known as 2,3-dicarboxypropylation or itaconation [13-16]. In response to inflammatory signals, the production of itaconate helps regulate the expression of inflammatory genes by modulating SDH and interfering with the glycolysis pathway through the alkylation of vital glycolytic enzymes like aldolase A (ALDOA) [17] and glyceraldehyde 3-phosphate dehydrogenase (GAPDH) [18] in immune cells. Itaconate also alkylates kelch-like ECH-associated protein 1 (KEAP1) and glutathione (GSH), distinguishing it as a potential activator of the master antioxidant regulator, nuclear factor erythroid 2-related factor 2 (NRF2), and as an inducer of the anti-inflammatory transcription factor, activating transcription factor 3 (ATF3) [15, 16]. Additionally, itaconate can inhibit the activation of the NLRP3 inflammasome to disrupt NLRP3-NEK7 interaction and modify Janus kinase 1 (JAK1) to suppress the alternative activation of macrophages [13, 14].

While a link between itaconate in the macrophage-associated inflammatory response and tumorigenesis has been proposed, the direct role of itaconate in breast tumorigenesis is currently unknown. Recent experimental mouse models utilizing ACOD1 gene-deficient myeloid cells have been shown to disturb immunosuppression, enhance anti-tumor immunity, and improve the efficacy of immune checkpoint therapies [19, 20]. However, the evidence that upon LPS activation, mouse macrophages produce an mM concentration of itaconate, compared to a μM concentration produced in human cells, has, thus far, provided a complex picture, mainly regarding the role of itaconate and development strategies to inhibit its production or effects within the human tumor microenvironment [10, 12, 21, 22]. The need for further research into the role of itaconate in human cancer cells is urgent and of utmost importance for advancing cancer research.

The extracellular signal-regulated kinase (ERK1/2) signal pathway is crucial in cell proliferation, differentiation, motility, and death [23-27] and holds significant potential in cancer treatment [28]. The ERK1/2 requires two critical phosphorylation of the TEY motif (Thr185/Tyr187 for ERK2 and Thr202/Tyr204 for ERK1) for full conformational activation, which is crucial for the function of enzymes and their sub-sequent involvement in nuclear shuttling for various cellular processes [25, 29, 30]. Over 40% of human cancers are associated with aberrant ERK pathway activation [31, 32]. Conversely, there is evidence that cancer cells are susceptible to hyperactivation of ERK1/2 phosphorylation, leading to apoptosis or senescence [27, 32-36]. However, this vulnerability of cancer cells is not fully understood [27, 32]. While inhibiting ERK1/2 activity by blocking upstream effectors such as RAF and MEK has been approved for cancer therapy, most ERK inhibitors are currently in clinical trials [33, 37]. Targeting the RTK/RAS/RAF pathway can enhance specific immune responses; the long-term effects should be carefully considered, as they may result in immunosuppression and promote tumor survival strategies [32, 38-40]. Notably, a novel concept is emerging: excessive activation of the ERK pathway can be lethal to cancer cells, offering a new and promising approach for cancer treatment through ERK pathway agonism [32-36].

Apoptosis inhibitor 5 (API5) is a nuclear protein that prevents cell death when cells are deprived of growth factors [41]. Although the precise mechanism remains unclear, research indicates that API5 suppresses E2F1-induced apoptosis and activates cell cycle-related genes [42-44]. API5 is often increased in various types of cancer, including breast cancer [45-47]. Elevated API5 expression is associated with tumor progression, metastasis, and resistance to conventional therapies, enabling cancer cells to evade apoptosis [46-49]. The structural elements of API5 protein function as protein-protein interaction modules, enabling API5 to interact with multiple binding partners and likely serve as a scaffold protein [42]. API5 has been found to interact with numerous components of large multi-protein complexes, including partners involved in apoptosis, cell survival, immune response, transcription, RNA export, and chromatin remodeling [43, 50]. The multifaceted roles and regulatory mechanisms of API5 in controlling cell fate decisions represent a significant and intriguing area of research in cancer biology.

Our current study investigated the potential of ITA as a promising therapeutic approach for tamoxifen-resistant breast cancer, focusing on the molecular mechanisms behind ITA's ability

to inhibit the growth of ER-positive breast cancer cells. We discovered that itaconate directly alkylates ERK2 at cysteine residue 254, leading to a substantial increase in ERK2 phosphorylation at the T185/Y187 sites and activity, which ultimately causes growth inhibition in ER-positive breast cancer cells. Moreover, itaconate inhibits the growth of tamoxifen-resistant cells by activating the ERK2 signal. Furthermore, activated ERK2 physically interacts with API5, disrupting API5's localization to the nuclear speckle, where it may interact with key molecules that regulate genes involved in cell growth.

In conclusion, our findings provide fundamental evidence supporting a novel therapeutic potential in which itaconate directly targets the ERK2 signaling pathway to suppress the growth of tamoxifen-sensitive and tamoxifen-resistant breast cancer cells.

Materials and methods

Cell culture

MCF7 (ATCC HTB-22) cells were grown in Minimum Essential Medium Eagle with Earle's Balanced Salts, supplemented with 2 mM L-glutamine, 1.5 g/L sodium bicarbonate, 0.1 mM non-essential amino acids, 1 mM sodium pyruvate, and 10% fetal bovine serum [51]. MCF7 Tam1 (ATCC CRL-3435) cells, resistant to tamoxifen, were cultured in Dulbecco's Minimum Essential Medium supplemented with 10 ng/mL human insulin, 1 μM 4-hydroxy-tamoxifen, and 10% fetal bovine serum. T47D (ATCC HTB-133) cells were grown in RPMI-1640 medium supplemented with 0.2 units/mL bovine insulin and 10% fetal bovine serum [51]. T47D Tam1 (ATCC CRL-3436) cells, also tamoxifen-resistant, were maintained in RPMI-1640 medium with 10 ng/mL human insulin, 1 μM 4-hydroxytamoxifen, and 10% fetal bovine serum.

Plasmids and transfection of cells

The MAPK1 (NM_138957) Human Tagged ORF Clone (RC204703) was obtained from OriGene Technologies, Inc. Mutant constructs were created using the QuikChange Lightning Site-Directed Mutagenesis Kit (210519, Agilent Technologies, Inc.) following the manufacturer's instructions. Stable transfections were conducted by introducing MAPK1_WT and mutant constructs into cells using the TransIT®-BrCa Transfection Reagent (MIR5500, Mirus Bio LLC). Stably transfected clones were selected with 0.2 mg/mL G418.

Clonogenic assays

2×10^3 of cells were seeded in 6-well plates and treated for 10-14 days with various concentrations of itaconate (I29204, Sigma-Aldrich) or 4-octyl-itaconate (25374, Cayman) in the presence or absence of 4-hydroxytamoxifen (H6278, Sigma-Aldrich). Then, cells were fixed with 4% formaldehyde overnight and stained with crystal violet (V5265, Sigma-Aldrich). The dye was thawed in 33% acetic acid, measuring at 595 nm absorbance using a Synergy H1 Hybrid Multi-Mode Reader (Agilent Technologies) [51].

Immunoprecipitation (IP)

Equal protein samples were immunoprecipitated using 40 μL of ANTI-FLAG® M2 Magnetic Beads (M8823, Merck) for 2 hours at 4°C. Following immunoprecipitation, the beads were thoroughly washed and boiled, and the resulting samples were analyzed by Western blotting.

Nucleus fraction

Nuclear fractions were extracted using the Nuclear Extraction Kit (ab113474, Abcam) following the manufacturer's protocol. Briefly, 5×10^7 cells were harvested in cytosol fractionation buffer supplemented with freshly prepared Phos-STOP Phosphatase (4906845001, Roche) and Protease Inhibitor Cocktail Tablets (5892970001, Roche). The suspension was set on ice for 10 minutes and vortexed for 10 seconds before centrifuging at 12,000 rpm for 1 minute [52]. The nuclear pellet obtained was resuspended in a nuclear fractionation buffer and incubated on ice for 15 minutes with intermittent vertexing, followed by centrifuging at 14,000 rpm for 10 minutes at 4°C. Western blot examined nuclear proteins using anti-API5 (25689-1-AP, Proteintech) for detection, with Lamin A/C (sc-376248, Santa Cruz Biotechnology) as the nuclear marker.

Western blotting analysis

Cells were lysed in RIPA buffer (R0278, Sigma-Aldrich) to obtain the lysates for subjecting to

Western blot analysis using specific primary antibodies. Protein bands were detected using fluorescent secondary antibodies and visualized with the ChemiDoc System (Bio-Rad Laboratories, Inc.). The primary antibodies included anti-phospho-ERK2 (T185/Y187) (MAB-1463, Abnova), ERK2 (#9108, Cell Signaling Technology), anti-GAPDH (sc-32233, Santa Cruz Biotechnology), anti-API5 (25689-1-AP, Proteintech), and anti-actin (66009-1-Ig, Proteintech).

Immunofluorescence staining

Cells were fixed with 4% paraformaldehyde (PFA) for 10 minutes at 4°C, followed by permeabilization with methanol for 10 minutes at -20°C [52]. Fixed and permeabilized cells were incubated overnight at 4°C with an anti-API5 antibody (25689-1-AP, Proteintech) diluted 1:200. Secondary detection was performed with Alexa Fluor 488-conjugated anti-rabbit antibody (A-11008, Thermo Scientific) at a 1:400 dilution for 1 hour at room temperature. For nuclear staining, slides were prepared with ProLong Gold Antifade Reagent (P36935, Thermo Fisher Scientific) containing DAPI. Imaging was conducted with a Leica TCS SP8 confocal microscope, and analysis was performed using ImageJ software with the JACoP plugin [53].

Proteomic identification, enrichment analysis, and identification of itaconation sites

Proteomic alterations in ITA-S and ITA-I cells were identified via mass spectrometry (MS). Total proteins were lysized using RIPA buffer; 40 µg protein was separated on a 10% SDS-PAGE gel for each sample and divided into five fractions. Gel slices (≤ 1 mm^3) were digested in gel to produce tryptic peptides. MS analysis was conducted on an Orbitrap Fusion mass spectrometer (Thermo Fisher Scientific), the Ultimate 3000 RSLC system (Dionex), and a nano-electrospray ion source. Full scans were acquired over an m/z range of 375-1,500 (AGC target: 4×10^5) at 120,000 resolution (m/z 200), with the 20 most abundant ions fragmented by collision-induced dissociation for tandem MS [51]. Protein identification and label-free quantification were conducted using Proteome Discoverer 2.4, with a significance threshold of P < 0.05. Enrichment analysis of the Kyoto Encyclopedia of Genes and Genomes (KEGG) pathways was performed using Shiny-

GO 0.77 [54]. Identification of itaconation sites employed LC-MS/MS data analyzed via Proteome Discoverer 2.4, incorporating static cysteine modification (+57.0215 Da) and variable modifications of +325.16378 Da (cysteine) and +382.18524 Da (lysine or histidine).

ERK2 interacting protein identification

Immunoprecipitation beads were mixed with SDS-PAGE buffer, heated at 95°C for 5 minutes, and proteins separated on a 12.5% polyacrylamide gel into five fractions. Gel pieces were digested with sequencing-grade trypsin at 37°C for 16 hours. Extracted peptides were dried, reconstituted in 0.1% formic acid, and analyzed by LC-MS/MS. Peptides were loaded onto a reverse-phase column, desalted, and separated over 70 minutes using a multi-step gradient at 0.3 µL/min. The LC system was coupled to an Orbitrap mass spectrometer operating at 120,000 resolution (m/z 400) with data-dependent acquisition of the 20 most abundant ions. Dynamic exclusion (40 s, ±15 ppm) and internal calibration (m/z 536.165365) were applied. Proteome Discoverer software with Mascot searches against SwissProt was used for data analysis, with 10 ppm precursor and 0.5 Da fragment mass tolerances, allowing two missed cleavages. High-confidence peptide-spectrum matches (PSMs) with < 1% FDR were retained. Single-peptide identifications were excluded, and relative quantification was performed using Minora. Proteins with $\geq$ 2-fold changes were identified as differentially expressed.

Statistical analysis

All graphs display the mean ± SEM from three independent assays. The Student's t-test was used to compare two groups, while one-way or two-way ANOVA was applied for comparisons involving three or more groups. A *p*-value of less than 0.05 was considered statistically significant. Statistical analyses were performed using Prism 9.0 software.

Results

Itaconate inhibits Tamoxifen (Tam)-resistant cell growth and enhances effectiveness in combination with Tam

Despite the initial success of tamoxifen treatment for most ER-positive breast cancers, a

significant percentage of tumors either exhibit intrinsic resistance or develop acquired resistance over time [3]. Our research has shown that exposure to itaconate (ITA) through external addition or internal production via enforced expression of ACOD1 leads to metabolic shifts, causing energy stress, cell cycle arrest, and cell apoptosis in ER-positive breast cancer cells [51].

To identify new therapeutic opportunities for ITA, we tested the response of MCF7 tamoxifen (Tam)-resistant cells (MCF7_Tam-R, Supplementary Figure 1A) to ITA and ITA's derivative, 4-octyl-itaconate (4-OI) stimulations. The dosages of ITA and 4-OI used were based on our previous report [51] and were lower than those used in most immune cell studies [10, 11, 15, 16]. Notably, MCF7 Tam-R cells displayed heightened sensitivity to doses of ITA at 0.25, 0.5, and 1 mM, as shown in **Figure 1A**. Also, 4-OI significantly inhibited cell growth at 31.3 and 62.5 µM concentrations compared to Tam-sensitive cells (MCF7_Tam-S), illustrated in **Figure 1B**. The combination of Tam and 4-OI notably enhanced growth inhibition in Tam-R cells, reducing their growth rate to about 30% with 7.8 µM 4-OI in the presence of 0.5 µM Tam. In comparison, about a 75% growth rate was observed with 4-OI alone (**Figure 1C**). In contrast, the combined effect was not seen in MCF7 Tam-S cells (Supplementary Figure 1B). Similar promising results were also observed in T47D tamoxifen-sensitive (T47D_Tam-S) and resistant cells (T47D_Tam-R) (**Figure 1D** and **1E**, Supplementary Figure 1C and 1D). Our findings highlight the potential of developing itaconate as a therapeutic option for treating Tam-resistant breast cancer, motivating further research in this area.

Itaconate activates ERK2 via alkylating on Cys 254 to inhibit ER-positive cancer cell growth

While ITA is recognized as an immunomodulatory metabolite linking metabolism and immune cell functions, its role in other cell types, especially in cancer cells, is still not fully understood. To further investigate the mechanisms underlying ITA's effects, we developed an ITA-insensitive cell line (ITA-I) that tolerates long-term exposure to endogenous ITA by forced expression of the ACOD1 gene in MCF7 cells (Supplementary Figure 2). The ITA-I cells exhibited more excellent resistance to treatments

with various concentrations of exogenous ITA (**Figure 2A**) and 4-OI (**Figure 2B**) compared to ITA-sensitive cells (ITA-S).

Using label-free quantitative proteomics, we compared differentially expressed proteins between the ITA-S and ITA-I groups based on a fold change of > 2 and *p*-values < 0.05, identifying 623 proteins - 326 of which were upregulated and 297 were downregulated, followed as determined through cluster analysis with KEGG database pathways using ShinyGO0.77 [54]. **Figure 2C** presents the top 3 significantly downregulated pathways; however, no upregulated pathways were detected. We have shown that ITA activates the AMP-activated protein kinase pathway in response to metabolic stress, leading to changes in glycolysis, the TCA cycle, and lipid metabolism in ITA-S cells [51]. In this study, we further explored the hypothesis that reduced MAPK/ERK signaling may contribute to the insensitivity of ITA observed in ITA-I cells, which could provide insights into the role of ITA in ER-positive breast cancer cell metabolism and signaling pathways.

Numerous studies have illustrated the ability of ITA and 4-OI to modify cysteine residues in a process known as 2,3-dicarboxypropylation or itaconation, thereby modulating the functions of target proteins [13-18]. Our comprehensive mass spectrometry analysis, a widely accepted method for protein identification and quantification, revealed 67 proteins with cysteine itaconation, with 37 showing increased itaconation and 30 showing decreased itaconation. Integrating itaconated proteome datasets allowed us to identify MAPK1/ERK2 as a potential target of ITA modification at cysteine residue 254 (**Figure 2D**). C254 residue is located in the C-terminal lobe of ERK2, which contains ERK2's activation and catalytic loop; thus, the significant decrease in ITA modification in ITA-I cells accompanied by downregulated MAPK/ERK signaling pathway implies that ITA may activate ERK2 via directly modify on Cys 254 residue to inhibit cell growth in ITA-S cells.

To demonstrate the impact of ITA alkylation on the cysteine residue 254 of ERK2, we created a flag-tagged wild-type ERK (ERK_WT) and a mutant resistant to ITA conjugation by substituting the cysteine residue with serine to explore cell growth in response to 4-OI stimulation. Our previous findings indicate that 4-OI
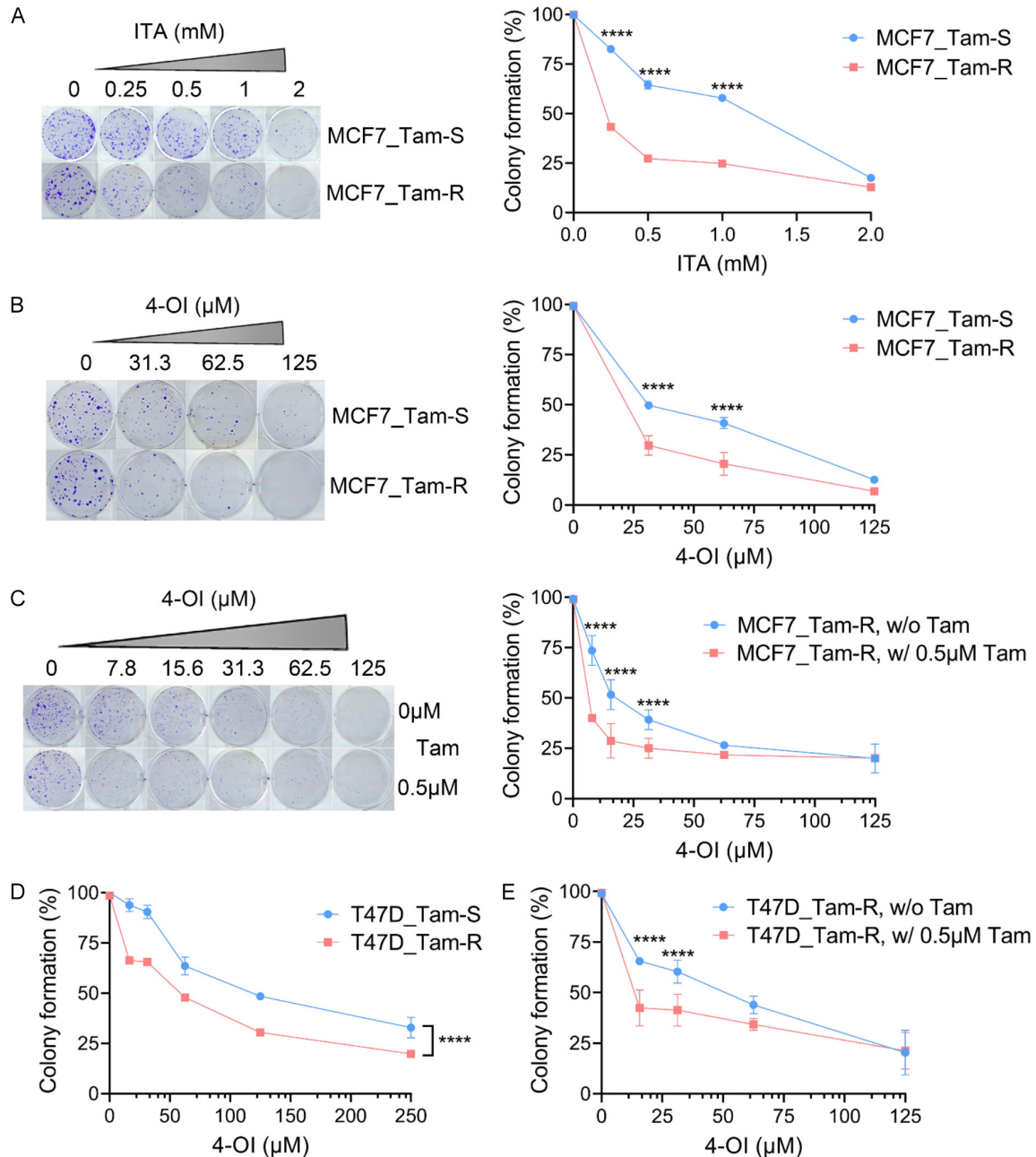
Figure 1. Itaconate inhibits tamoxifen-resistant ER-positive breast cancer cell growth. The colony formation of various doses of (A) itaconate (ITA), (B) 4-octyl-itaconate-(4-OI), and (C) 4-OI in combination with 0.5 μM 4-OH-tamoxifen treated MCF7 tamoxifen-sensitive (Tam-S) and tamoxifen-resistant (Tam-R) cells for fourteen days. An equal volume of the medium as control. (D) and (E) T47D tamoxifen-sensitive (Tam-S) and tamoxifen-resistant (Tam-R) cells were treated as described in (B) and (C) for growth assay. Representative images and the data are shown as mean ± SEM from three experiments. ****P < 0.0001 among groups; two-way ANOVA.

inhibits the growth of ER-positive breast cancer cells [51] (**Figure 3A**). Notably, ERK2_WT cells exhibited heightened sensitivity to 4-OI compared to the vector control cells (**Figure 3A**). In contrast, ERK2_C254S cells demonstrated increased resistance to the 4-OI's inhibitory effects at various doses (**Figure 3A**), highlighting the necessity of Cys 254 alkylation for the growth-inhibitory effect of 4-OI. The T185 residue of ERK2 is critical for stabilizing the conformation of the catalytic site. As expected, a non-phosphorylation-mimic ERK2 mutant, ERK2_
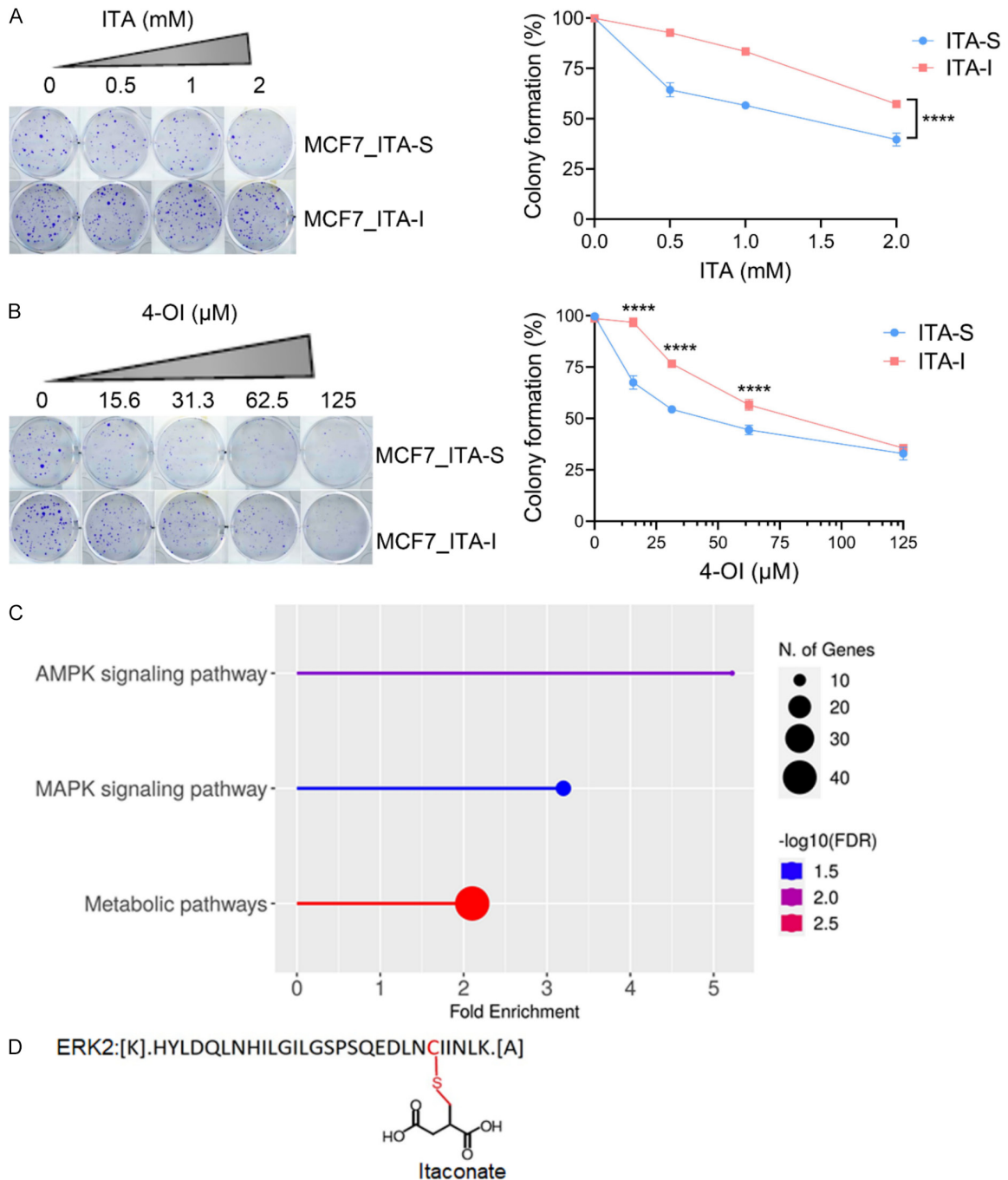
Figure 2. MAPK signaling is down-regulated in itaconate-insensitive ER-positive breast cancer cells. The colony formation of various doses of (A) ITA and (B) 4-OI treated ITA-S (ITA-sensitive) and ITA-I (ITA-insensitive) cells for ten days - an equal medium volume as control. Representative images and the data are shown as mean ± SEM from three experiments. ****$P < 0.0001$ between ITA-S and ITA-I cells; two-way ANOVA. (C) Kyoto Encyclopedia of Genes and Genomes (KEGG) pathway enrichment analysis based on the differentially expressed proteins of ITA-S and ITA-I cells ($P < 0.05$). (D) Schematics of the itaconated ERK2 peptide structure on Cys_254.

T185Q, also potentially impeded the 4-OI's effect on ER-positive breast cancer cell growth (**Figure 3A**), further supporting the notion that the phosphorylation at TEY motif and activation of ERK2 are required for 4-OI to inhibit cell growth.
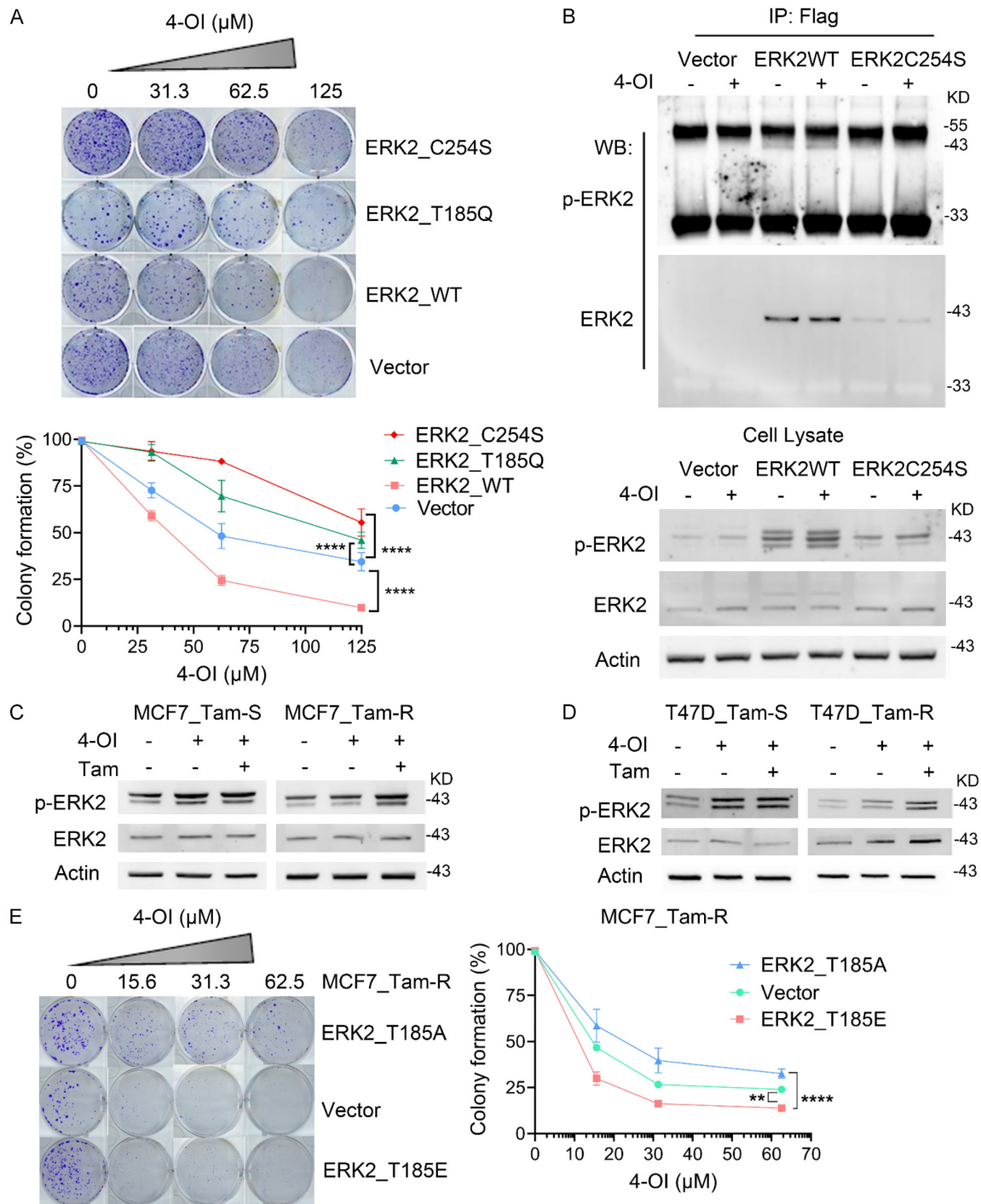
Figure 3. Itaconate conjugation at the Cys_254 residue of ERK2 inhibits the growth of ER-positive breast cancer cells. (A) Colony formation assay of MCF7 cells treated with 4-OI, featuring Vector, ERK2_WT, ERK2_C254S, and ERK2_T185Q expressions for ten days. An equal volume of medium was used as the control. Representative images and data as mean ± SEM. Statistical significance was determined with ****P < 0.0001 among groups; two-way ANOVA. Western blot analysis of phosphorylated TEY motif of ERK2 in (B) MCF7 cells expressing Vector, ERK2_WT, and ERK2_C254S, following immunoprecipitation with the flag antibody, (C) MCF7_Tam-S cells treated with 50 μM 4-OI alone or in combination with 0.5 μM 4-OH tamoxifen for 4 hours or MCF7_Tam-R for 16 hours, and (D) T47D_Tam-S cells treated with 50μM 4-OI alone or in combination with 0.5 μM 4-OH tamoxifen for 4 hours or T47D_Tam-R for 16 hours. (E) Colony formation assay of 4-OI-treated MCF7_Tam-R cells expressing Vector, ERK2_T185E, and ERK2_T185A for fourteen days. An equal volume of medium was used as the control. Three independent experiments present Representative images and data as mean ± SEM. Statistical significance was determined with ****P < 0.0001 among groups; two-way ANOVA.

When we immunoprecipitated ERK2 proteins using an anti-flag antibody, we observed a phosphorylated form at the TEY motif of full-length ERK2 in the ERK2_WT expressing cells, both with and without 4-OI treatment. This phenomenon was absent in the C254S and T185Q mutant cells (**Figure 3B** and Supplementary Figure 3A). Furthermore, we detected elevated ERK2 phosphorylation levels at the TEY motif in the input cell lysate of vector cells treated with 50 μM of 4-OI for 4 hours, compared to vehicle-treated cells. Cells expressing ERK2_WT showed significantly enhanced phosphorylation at the TEY motif even without 4-OI treatment. In contrast, the ERK2_C254S mutant displayed a marked decrease in phosphorylation levels compared to the wild type, although some endogenous phosphorylation of ERK2 was still detected (**Figure 3B** and Supplementary Figure 3B). Our data indicate that ITA directly modifies cysteine residue 254, leading to increased ERK2 phosphorylation at the TEY motif and consequently inhibiting cell growth in ER-positive breast cancer cells.

Itaconate enhances ERK2 activation to inhibit the growth of Tamoxifen-resistant cells

It was noted that tamoxifen induces cell death by activating the ERK1/2 signaling pathway, an effect that estrogen agonists cannot counter [55]. The individual administration of ITA caused ERK2 phosphorylation at the TEY motif in MCF7 and T47D Tam-S cells (**Figure 3C** and **3D**, Supplementary Figure 3C and 3D); its combination with tamoxifen further amplified this effect in tamoxifen-resistant cells (**Figure 3C** and **3D**, Supplementary Figure 3C and 3D). These findings were consistent with ITA's function on cell growth inhibition (**Figure 1** and Supplementary Figure 1), suggesting the potential of ITA to upregulate ERK2 activity and effectively impede the growth of tamoxifen-resistant ER-positive breast cancer cells.

To further demonstrate the phosphorylation at the TEY motif and activation of ERK2 are required for 4-OI to inhibit tamoxifen-resistant cell growth, we generated a phosphorylation-mimic ERK2 mutant, ERK2_T185E and a non-phosphorylation-mimic ERK2 mutant, ERK2_T185A to see their growth response to ITA. Indeed, compared to the vector control cells, the ERK2_T185E cells exhibited enhanced sen-

sitivity to 4-OI, whose effect was reversed in ERK2_T185A cells (**Figure 3E** and Supplementary Figure 3E). These data suggest that 4-OI inhibits tamoxifen-resistant cell growth via increasing phosphorylation at the TEY motif and activation of ERK2, opening new possibilities for developing targeted cancer therapies.

Activated ERK2 interacts physically with API5 to disrupt API5's localization of the nucleus speckle

To understand the downstream effectors of ERK2 signaling with ITA modification, we conducted a comprehensive process that involved pulling down ERK2 to identify its associated proteins using label-free quantitative differential LC/MS/MS. We identified 379 proteins in the ERK2_WT group and 396 in the ERK_C254S group. Of these, 15 proteins were exclusively observed in the WT group; in comparison, 32 were unique to the mutant group (**Figure 4A**). Among the 15 interacting proteins from the ERK2_WT group, only the expression of API5 demonstrated a strong correlation (r > 0.7) with MAPK1/ERK2 gene expression in breast tumors (**Figure 4B**). Similar to the MAPK1/ERK2 gene expression patterns observed in the GEPIA analysis of the TCGA and GTEx databases (http://gepia.cancer-pku.cn) [56, 57], the elevated expression levels of API5 were also found in breast tumors compared to normal tissue (**Figure 4C**). Therefore, we focused on the role of API5 in the ITA/ERK2 axis regarding cell growth inhibition in ER-positive breast cancer.

API5 has been shown to play a crucial role in activating the transcription of cell cycle-associated genes through E2F1 by facilitating its recruitment to target promoters to enhance the transcription of genes regulated by E2F1 [58]. We hypothesized that the localization of API5 in the nucleus is essential for its function and interactions with other molecules that regulate genes involved in cell growth. To investigate this, we extracted nuclear fractions from cells expressing either the vector, ERK2_WT, C254S, or T185Q, with or without stimulation by 4-OI. We then performed Western blot analysis to detect API5 using a specific antibody. The result indicates that cells with ERK2_WT exhibited higher levels of nuclear API5 than the vector control. In contrast, cells expressing ERK_
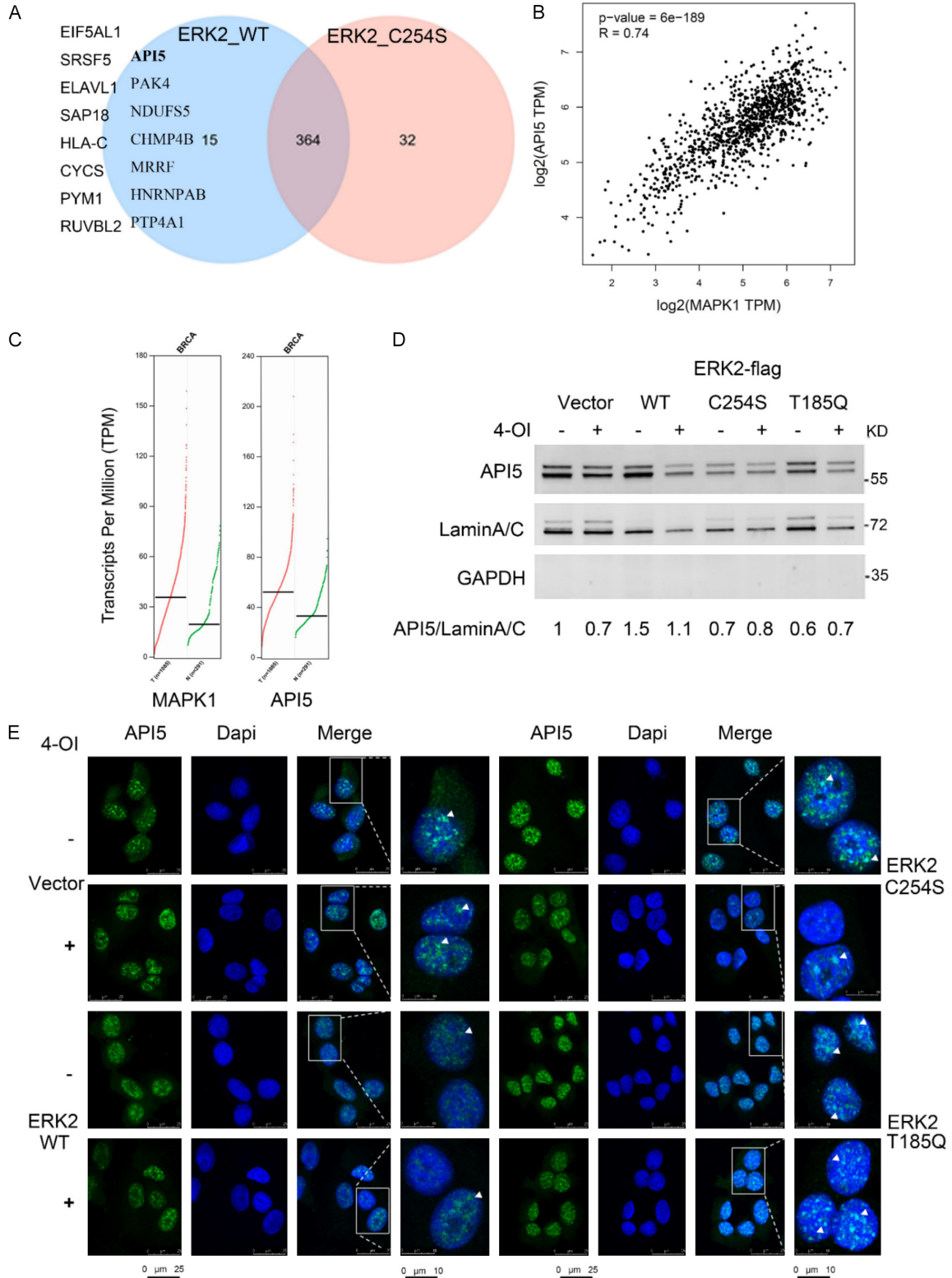
Figure 4. The nucleus distribution of API5 and its interaction with ERK2 depends on ERK2 activity. A. Venn diagram showing immunoprecipitation-based mass spectrometry identification of ERK2-interacting proteins in ERK2_WT and ERK2_C254S MCF7 cells. B. Spearman's correlation analysis reveals gene expression levels of API5 and ERK2 in breast cancer patients from the TGCA dataset within the GEPIA database. Spearman's correlation coefficient (r) and *p*-values are shown for analysis. C. The gene expression profiles in the breast cancer dataset within

the GEPIA database (http://gepia.cancer-pku.cn/[56, 57]). Red, tumor (n=1085); green, match TGCA normal and GTEX data (n=291). D. Analysis of nucleus API5 using Western blotting in MCF7 cells expressing Vector, ERK2_WT, ERK2_C254S, and ERK2_T185Q, following nucleus fraction extraction. LaminA/C, a nucleus marker; GAPDH, a cytosol marker. E. Representative confocal imaging of API5 (green) localization in the nucleus (blue) in MCF7 Vector, ERK2_WT, ERK2_C254S, and ERK2_T2185Q expressing cells with vehicle control or 50 μM 4-OI treatment for 2 days. Scale bars, 25 μm; A higher magnification of the insert: arrowhead, nuclear speckle. Scale bars, 10 μm.

C254S and T185Q showed reduced levels of nuclear API5 (**Figure 4D**). Moreover, stimulation with 4-OI led to a decrease in nuclear API5 levels in both vector and ERK2_WT cells, with no further reduction observed in cells expressing ERK2_C254 and ERK_T185Q.

Accordingly, API5 localized primarily within the nucleus in all experimental groups, as detected by fluorescent staining using a specific API5 antibody (**Figure 4E** and Supplementary Figure 4). Interestingly, in the vector control group, where cells were not treated with 4-OI, API5 was found in the nuclear speckle, a region known to enhance gene expression [59]. Following stimulation with 4-OI for 48 hours, the size of the nuclear speckle was reduced (**Figure 4E**). Notably, excessive activation of ERK2 disrupted the formation of this nuclear speckle, both in the absence and presence of 4-OI (**Figure 4E**). Conversely, ERK2_C254S cells showed an increased localization of API5 to nuclear speckles compared to control cells, even though 4-OI treatment reduced nuclear speckle localization (**Figure 4E**). Also, T185Q cells displayed enhanced localization of API5 to nuclear speckles and exhibited more excellent resistance to the disruption of nuclear speckle formation caused by 4-OI (**Figure 4E**). These findings highlight the critical role of tightly regulating ERK2 phosphorylation at TEY and its activity, which controls the nuclear speckle localization of API5, leading to modulating the genetic processes involved in cell growth [58].

Discussion

Our current study explored the potential of itaconate (ITA) as a promising therapeutic approach for treating tamoxifen-resistant breast cancer and the molecular mechanisms that enable ITA to inhibit the growth of the cells. Recent evidence suggests that the ACOD1 deletion with animal models reduces immunosuppression and augments cancer's immune checkpoint blockade (ICB) response, which discovery positions ACOD1 as a significant drug target in tumor immunology [19, 20]. However,

the ACOD1's potential goes beyond its enzymatic effects, and further investigation is needed to understand the role of ITA accumulation in tumor tissue in driving immunosuppression [21, 22].

Schofield et al. found that ICB-resistant prostate cancer cells exhibit high expressions of ACOD1, which hinders the proliferation of naïve CD8+ T cells, and this hindrance can be reversed by deleting ACOD1 [60]. Interestingly, suppressing CD8+ T cell proliferation does not depend on ITA secretion [60]. Despite detecting high ITA levels in ICB-resistant prostate cancer cells, it is still unclear how responsive they are to ITA, given its functional metabolite nature. Our ITA-insensitive ER-positive breast cancer cells showed high ACOD1 expression and ITA levels (**Figure 2A** and **2B**, Supplementary Figure 2), raising the question of whether ICB-resistant prostate cancer cells may also develop insensitivity to ITA during the acquisition of ICB resistance. These findings highlight the necessity for further research into the role of ITA in cancer cells, especially with immune checkpoint blockade (ICB) resistance [21, 22].

The ERK signaling pathway is essential for various cellular functions, making its regulation critical for appropriate cellular responses through post-translational modifications (PTMs) such as phosphorylation [23, 24, 26, 27]. While itaconate has been shown to signal via the G protein-coupled receptor oxoglutarate receptor 1 (OXGR1), inducing Ca^{2+} mobilization and ERK phosphorylation [61], our study identified a novel PTM for ERK2 through direct ITA alkylation at the C254 residue. This discovery opens exciting possibilities for precisely modulating ERK2's role in cellular signaling pathways. ERK C254 residue has also been shown to be subject to S-acylation, a reversible lipid modification, upon epidermal growth factor stimulation [62]. Unlike direct ITA conjugation, which does not involve enzymes, the S-acylation of ERK2 is regulated by "writer" proteins known as acyl transferases (PATs) and "eraser" proteins called acyl protein thioesterases (APTs) [62]. It

remains to be determined whether itaconate competes with lipids for binding to the C254 residue of ERK2 and what kind of upstream signals and signal magnitudes influence which PTM activates ERK2.

Cancer cells often depend on activating specific signaling pathways for survival. However, excessive activation of critical pathways like ERK can push these cells into stress, ultimately leading to cell death. Several studies have shown that enhancing ERK activity can induce apoptosis or senescence in cancer cells, particularly those with ERK mutations, suggesting that excessive activation of the ERK pathway can be detrimental to cancer cells [27, 32-36]. Our study has demonstrated a positive relationship between the expression of ERK2 and API5 in breast cancer patients (**Figure 4B**) and the ER-positive breast cancer cell line (**Figure 4D**). The result is consistent with previous reports that API5 overexpression enhances ERK2 protein expression in a cervical tumor cell line [63], suggesting the existence of a complex regulatory loop between ERK2 and API5. Understanding the intricate molecular mechanisms of the ERK2/API5 axis is essential for elucidating how ERK2 signaling transitions from promoting cell survival to triggering cell death.

Overall, the study grew our understanding of the role of itaconate in regulating ERK2 signal transduction and determined the fate of tamoxifen-sensitive and resistant breast cancer cells. Our findings suggest a new treatment strategy for cancer that focuses on activating the ERK pathway instead of inhibiting it, offering renewed hope for future cancer therapies.

Limitations of the study

The phosphorylation of ERK at its TEY motif is essential for its translocation to the nucleus, where ERK2 plays a crucial role in regulating gene expression. However, we must clarify how and where ERK2 interacts with API5 following ITA stimulation, which is central to understanding the ITA/ERK/API5 pathway. Unfortunately, our progress in this crucial area of research has been hindered by the lack of specific commercial antibodies for phospho-ERK2 and itaconated ERK2, which are necessary for conducting in situ proximity ligation assays. While one promising area to explore is the phosphorylated form of ERK2 as a specific biomarker to gauge the effectiveness of ITA therapy in ER-positive breast cancer patients, warrants further pursuit, we need to evaluate the ITA/ERK2/API5 axis using preclinical animal models. These models will enable the evaluation of ITA therapy in vivo and provide deeper insights into the contribution of the ITA/ERK2/API5 pathway to breast cancer progression.

Disclosure of conflict of interest

None.

Address correspondence to: Drs. Mien-Chie Hung and Hsueh-Chun Wang, Graduate Institute of Biomedical Sciences, China Medical University, No. 100, Section 1, Jingmao Road, Beitun District, Taichung, Taiwan. Tel: +886-4-22057153; Fax: +886-4-22952121; E-mail: mhung@mail.cmu.edu.tw; mhung77030@gmail.com (MCH); Tel: +886-4-22053366 Ext. 6735; Fax: +886-4-22333641; E-mail: hcwang1110@mail.cmu.edu.tw; hcwang1110@gmail.com (HCW)

References

[1] Scabia V, Ayyanan A, De Martino F, Agnoletto A, Battista L, Laszlo C, Treboux A, Zaman K, Stravodimou A, Jallut D, Fiche M, Bucher P, Ambrosini G, Sflomos G and Brisken C. Estrogen receptor positive breast cancers have patient specific hormone sensitivities and rely on progesterone receptor. Nat Commun 2022; 13: 3127.

[2] Hultsch S, Kankainen M, Paavolainen L, Kovanen RM, Ikonen E, Kangaspeska S, Pietiainen V and Kallioniemi O. Association of tamoxifen resistance and lipid reprogramming in breast cancer. BMC Cancer 2018; 18: 850.

[3] Lei JT, Anurag M, Haricharan S, Gou X and Ellis MJ. Endocrine therapy resistance: new insights. Breast 2019; 48: S26-S30.

[4] Yin L, Pan X, Zhang XT, Guo YM, Wang ZY, Gong Y and Wang M. Downregulation of ER-alpha36 expression sensitizes HER2 overexpressing breast cancer cells to tamoxifen. Am J Cancer Res 2015; 5: 530-544.

[5] Jeong D, Ham J, Kim HW, Kim H, Ji HW, Yun SH, Park JE, Lee KS, Jo H, Han JH, Jung SY, Lee S, Lee ES, Kang HS and Kim SJ. ELOVL2: a novel tumor suppressor attenuating tamoxifen resistance in breast cancer. Am J Cancer Res 2021; 11: 2568-2589.

[6] van der Willik KD, Timmermans MM, van Deurzen CH, Look MP, Reijm EA, van Zundert WJ, Foekens R, Trapman-Jansen AM, den Bakker MA, Westenend PJ, Martens JW, Berns EM and Jansen MP. SIAH2 protein expression in breast cancer is inversely related with ER status and outcome to tamoxifen therapy. Am J Cancer Res 2016; 6: 270-284.

[7] Ryan DG, Murphy MP, Frezza C, Prag HA, Chouchani ET, O'Neill LA and Mills EL. Coupling Krebs cycle metabolites to signalling in immunity and cancer. Nat Metab 2019; 1: 16-33.

[8] Pavlova NN, Zhu J and Thompson CB. The hallmarks of cancer metabolism: still emerging. Cell Metab 2022; 34: 355-377.

[9] Martinez-Reyes I and Chandel NS. Cancer metabolism: looking forward. Nat Rev Cancer 2021; 21: 669-680.

[10] Cordes T, Wallace M, Michelucci A, Divakaruni AS, Sapcariu SC, Sousa C, Koseki H, Cabrales P, Murphy AN, Hiller K and Metallo CM. Immunoresponsive gene 1 and itaconate inhibit succinate dehydrogenase to modulate intracellular succinate levels. J Biol Chem 2016; 291: 14274-14284.

[11] Lampropoulou V, Sergushichev A, Bambouskova M, Nair S, Vincent EE, Loginicheva E, Cervantes-Barragan L, Ma X, Huang SC, Griss T, Weinheimer CJ, Khader S, Randolph GJ, Pearce EJ, Jones RG, Diwan A, Diamond MS and Artyomov MN. Itaconate links inhibition of succinate dehydrogenase with macrophage metabolic remodeling and regulation of inflammation. Cell Metab 2016; 24: 158-166.

[12] Michelucci A, Cordes T, Ghelfi J, Pailot A, Reiling N, Goldmann O, Binz T, Wegner A, Tallam A, Rausell A, Buttini M, Linster CL, Medina E, Balling R and Hiller K. Immune-responsive gene 1 protein links metabolism to immunity by catalyzing itaconic acid production. Proc Natl Acad Sci U S A 2013; 110: 7820-7825.

[13] Hooftman A, Angiari S, Hester S, Corcoran SE, Runtsch MC, Ling C, Ruzek MC, Slivka PF, McGettrick AF, Banahan K, Hughes MM, Irvine AD, Fischer R and O'Neill LAJ. The immunomodulatory metabolite itaconate modifies NLRP3 and inhibits inflammasome activation. Cell Metab 2020; 32: 468-478.

[14] Runtsch MC, Angiari S, Hooftman A, Wadhwa R, Zhang Y, Zheng Y, Spina JS, Ruzek MC, Argiriadi MA, McGettrick AF, Mendez RS, Zotta A, Peace CG, Walsh A, Chirillo R, Hams E, Fallon PG, Jayamaran R, Dua K, Brown AC, Kim RY, Horvat JC, Hansbro PM, Wang C and O'Neill LAJ. Itaconate and itaconate derivatives target JAK1 to suppress alternative activation of macrophages. Cell Metab 2022; 34: 487-501.

[15] Mills EL, Ryan DG, Prag HA, Dikovskaya D, Menon D, Zaslona Z, Jedrychowski MP, Costa ASH, Higgins M, Hams E, Szpyt J, Runtsch MC, King MS, McGouran JF, Fischer R, Kessler BM, McGettrick AF, Hughes MM, Carroll RG, Booty LM, Knatko EV, Meakin PJ, Ashford MLJ, Modis LK, Brunori G, Sevin DC, Fallon PG, Caldwell ST, Kunji ERS, Chouchani ET, Frezza C, Dinkova-Kostova AT, Hartley RC, Murphy MP and O'Neill LA. Itaconate is an anti-inflammatory metabolite that activates Nrf2 via alkylation of KEAP1. Nature 2018; 556: 113-117.

[16] Bambouskova M, Gorvel L, Lampropoulou V, Sergushichev A, Loginicheva E, Johnson K, Korenfeld D, Mathyer ME, Kim H, Huang LH, Duncan D, Bregman H, Keskin A, Santeford A, Apte RS, Sehgal R, Johnson B, Amarasinghe GK, Soares MP, Satoh T, Akira S, Hai T, de Guzman Strong C, Auclair K, Roddy TP, Biller SA, Jovanovic M, Klechevsky E, Stewart KM, Randolph GJ and Artyomov MN. Electrophilic properties of itaconate and derivatives regulate the IkappaBzeta-ATF3 inflammatory axis. Nature 2018; 556: 501-504.

[17] Qin W, Qin K, Zhang Y, Jia W, Chen Y, Cheng B, Peng L, Chen N, Liu Y, Zhou W, Wang YL, Chen X and Wang C. S-glycosylation-based cysteine profiling reveals regulation of glycolysis by itaconate. Nat Chem Biol 2019; 15: 983-991.

[18] Liao ST, Han C, Xu DQ, Fu XW, Wang JS and Kong LY. 4-Octyl itaconate inhibits aerobic glycolysis by targeting GAPDH to exert anti-inflammatory effects. Nat Commun 2019; 10: 5091.

[19] Zhao H, Teng D, Yang L, Xu X, Chen J, Jiang T, Feng AY, Zhang Y, Frederick DT, Gu L, Cai L, Asara JM, Pasca di Magliano M, Boland GM, Flaherty KT, Swanson KD, Liu D, Rabinowitz JD and Zheng B. Myeloid-derived itaconate suppresses cytotoxic CD8(+) T cells and promotes tumour growth. Nat Metab 2022; 4: 1660-1673.

[20] Chen YJ, Li GN, Li XJ, Wei LX, Fu MJ, Cheng ZL, Yang Z, Zhu GQ, Wang XD, Zhang C, Zhang JY, Sun YP, Saiyin H, Zhang J, Liu WR, Zhu WW, Guan KL, Xiong Y, Yang Y, Ye D and Chen LL. Targeting IRG1 reverses the immunosuppressive function of tumor-associated macrophages and enhances cancer immunotherapy. Sci Adv 2023; 9: eadg0654.

[21] Waqas FH, Chen C and Pessler F. Aconitate decarboxylase (ACOD1) has found a disease. Trends Endocrinol Metab 2024; 35: 561-562.

[22] McGettrick AF, Bourner LA, Dorsey FC and O'Neill LAJ. Metabolic messengers: itaconate. Nat Metab 2024; 6: 1661-1667.

[23] Roux PP and Blenis J. ERK and p38 MAPK-activated protein kinases: a family of protein kinases with diverse biological functions. Microbiol Mol Biol Rev 2004; 68: 320-344.

[24] Yoon S and Seger R. The extracellular signal-regulated kinase: multiple substrates regulate diverse cellular functions. Growth Factors 2006; 24: 21-44.

[25] Kennedy EP and Weiss SB. The function of cytidine coenzymes in the biosynthesis of phospholipides. J Biol Chem 1956; 222: 193-214.

[26] Sun Y, Liu WZ, Liu T, Feng X, Yang N and Zhou HF. Signaling pathway of MAPK/ERK in cell proliferation, differentiation, migration, senescence and apoptosis. J Recept Signal Transduct Res 2015; 35: 600-604.

[27] Lavoie H, Gagnon J and Therrien M. ERK signalling: a master regulator of cell behaviour, life and fate. Nat Rev Mol Cell Biol 2020; 21: 607-632.

[28] Roberts PJ and Der CJ. Targeting the Raf-MEK-ERK mitogen-activated protein kinase cascade for the treatment of cancer. Oncogene 2007; 26: 3291-3310.

[29] Canagarajah BJ, Khokhlatchev A, Cobb MH and Goldsmith EJ. Activation mechanism of the MAP kinase ERK2 by dual phosphorylation. Cell 1997; 90: 859-869.

[30] Ebisuya M, Kondoh K and Nishida E. The duration, magnitude and compartmentalization of ERK MAP kinase activity: mechanisms for providing signaling specificity. J Cell Sci 2005; 118: 2997-3002.

[31] Lee S, Rauch J and Kolch W. Targeting MAPK signaling in cancer: mechanisms of drug resistance and sensitivity. Int J Mol Sci 2020; 21: 1102.

[32] Timofeev O, Giron P, Lawo S, Pichler M and Noeparast M. ERK pathway agonism for cancer therapy: evidence, insights, and a target discovery framework. NPJ Precis Oncol 2024; 8: 70.

[33] Sammons RM, Ghose R, Tsai KY and Dalby KN. Targeting ERK beyond the boundaries of the kinase active site in melanoma. Mol Carcinog 2019; 58: 1551-1570.

[34] Satoh R, Hamada N, Yamada A, Kanda Y, Ishikawa F, Takasaki T, Tanabe G and Sugiura R. Discovery of new benzhydrol biscarbonate esters as potent and selective apoptosis inducers of human melanomas bearing the activated ERK pathway: SAR studies on an ERK MAPK signaling modulator, ACA-28. Bioorg Chem 2020; 103: 104137.

[35] Satoh R, Hagihara K, Matsuura K, Manse Y, Kita A, Kunoh T, Masuko T, Moriyama M, Moriyama H, Tanabe G, Muraoka O and Sugiura R. Identification of ACA-28, a 1'-acetoxychavicol acetate analogue compound, as a novel modulator of ERK MAPK signaling, which preferentially kills human melanoma cells. Genes Cells 2017; 22: 608-618.

[36] Sugiura R, Satoh R and Takasaki T. ERK: a double-edged sword in cancer. ERK-dependent apoptosis as a potential therapeutic strategy for cancer. Cells 2021; 10: 2509.

[37] Roskoski R Jr. ERK1/2 MAP kinases: structure, function, and regulation. Pharmacol Res 2012; 66: 105-143.

[38] Yang L, Zheng L, Chng WJ and Ding JL. Comprehensive analysis of ERK1/2 substrates for potential combination immunotherapies. Trends Pharmacol Sci 2019; 40: 897-910.

[39] Prasad M, Zorea J, Jagadeeshan S, Shnerb AB, Mathukkada S, Bouaoud J, Michon L, Novoplansky O, Badarni M, Cohen L, Yegodayev KM, Tzadok S, Rotblat B, Brezina L, Mock A, Karabajakian A, Fayette J, Cohen I, Cooks T, Allon I, Dimitstein O, Joshua B, Kong D, Voronov E, Scaltriti M, Carmi Y, Conde-Lopez C, Hess J, Kurth I, Morris LGT, Saintigny P and Elkabets M. MEK1/2 inhibition transiently alters the tumor immune microenvironment to enhance immunotherapy efficacy against head and neck cancer. J Immunother Cancer 2022; 10: e003917.

[40] Coelho MA, de Carne Trecesson S, Rana S, Zecchin D, Moore C, Molina-Arcas M, East P, Spencer-Dene B, Nye E, Barnouin K, Snijders AP, Lai WS, Blackshear PJ and Downward J. Oncogenic RAS signaling promotes tumor immunoresistance by stabilizing PD-L1 mRNA. Immunity 2017; 47: 1083-1099.

[41] Tewari M, Yu M, Ross B, Dean C, Giordano A and Rubin R. AAC-11, a novel cDNA that inhibits apoptosis after growth factor withdrawal. Cancer Res 1997; 57: 4063-4069.

[42] Han BG, Kim KH, Lee SJ, Jeong KC, Cho JW, Noh KH, Kim TW, Kim SJ, Yoon HJ, Suh SW, Lee S and Lee BI. Helical repeat structure of apoptosis inhibitor 5 reveals protein-protein interaction modules. J Biol Chem 2012; 287: 10727-10737.

[43] Abbas H, Derkaoui DK, Jeammet L, Adiceam E, Tiollier J, Sicard H, Braun T and Poyet JL. Apoptosis inhibitor 5: a multifaceted regulator of cell fate. Biomolecules 2024; 14: 136.

[44] Imre G, Berthelet J, Heering J, Kehrloesser S, Melzer IM, Lee BI, Thiede B, Dotsch V and Rajalingam K. Apoptosis inhibitor 5 is an endogenous inhibitor of caspase-2. EMBO Rep 2017; 18: 733-744.

[45] Kuttanamkuzhi A, Panda D, Malaviya R, Gaidhani G and Lahiri M. Altered expression of

anti-apoptotic protein Api5 affects breast tumorigenesis. BMC Cancer 2023; 23: 374.

[46] Noh KH, Kim SH, Kim JH, Song KH, Lee YH, Kang TH, Han HD, Sood AK, Ng J, Kim K, Sonn CH, Kumar V, Yee C, Lee KM and Kim TW. API5 confers tumoral immune escape through FGF2-dependent cell survival pathway. Cancer Res 2014; 74: 3556-3566.

[47] Cho H, Chung JY, Song KH, Noh KH, Kim BW, Chung EJ, Ylaya K, Kim JH, Kim TW, Hewitt SM and Kim JH. Apoptosis inhibitor-5 overexpression is associated with tumor progression and poor prognosis in patients with cervical cancer. BMC Cancer 2014; 14: 545.

[48] Kim JW, Cho HS, Kim JH, Hur SY, Kim TE, Lee JM, Kim IK and Namkoong SE. AAC-11 overexpression induces invasion and protects cervical cancer cells from apoptosis. Lab Invest 2000; 80: 587-594.

[49] Jang HS, Woo SR, Song KH, Cho H, Chay DB, Hong SO, Lee HJ, Oh SJ, Chung JY, Kim JH and Kim TW. API5 induces cisplatin resistance through FGFR signaling in human cancer cells. Exp Mol Med 2017; 49: e374.

[50] Bong SM, Bae SH, Song B, Gwak H, Yang SW, Kim S, Nam S, Rajalingam K, Oh SJ, Kim TW, Park S, Jang H and Lee BI. Regulation of mRNA export through API5 and nuclear FGF2 interaction. Nucleic Acids Res 2020; 48: 6340-6352.

[51] Wang HC, Chang WC, Lee DY, Li XG and Hung MC. IRG1/Itaconate induces metabolic reprogramming to suppress ER-positive breast cancer cell growth. Am J Cancer Res 2023; 13: 1067-1081.

[52] Wang HC, Liu KY, Wang LT, Hsu SH, Wang SC and Huang SK. Aryl hydrocarbon receptor promotes lipid droplet biogenesis and metabolic shift in respiratory Club cells. Hum Cell 2021; 34: 785-799.

[53] Bolte S and Cordelieres FP. A guided tour into subcellular colocalization analysis in light microscopy. J Microsc 2006; 224: 213-232.

[54] Ge SX, Jung D and Yao R. ShinyGO: a graphical gene-set enrichment tool for animals and plants. Bioinformatics 2020; 36: 2628-2629.

[55] Zheng A, Kallio A and Harkonen P. Tamoxifen-induced rapid death of MCF-7 breast cancer cells is mediated via extracellularly signal-regulated kinase signaling and can be abrogated by estrogen. Endocrinology 2007; 148: 2764-2777.

[56] Tang Z, Li C, Kang B, Gao G, Li C and Zhang Z. GEPIA: a web server for cancer and normal gene expression profiling and interactive analyses. Nucleic Acids Res 2017; 45: W98-W102.

[57] Tang Z, Kang B, Li C, Chen T and Zhang Z. GEPIA2: an enhanced web server for large-scale expression profiling and interactive analysis. Nucleic Acids Res 2019; 47: W556-W560.

[58] Garcia-Jove Navarro M, Basset C, Arcondeguy T, Touriol C, Perez G, Prats H and Lacazette E. Api5 contributes to E2F1 control of the G1/S cell cycle phase transition. PLoS One 2013; 8: e71443.

[59] Ilik IA and Aktas T. Nuclear speckles: dynamic hubs of gene expression regulation. FEBS J 2022; 289: 7234-7245.

[60] Schofield JH, Longo J, Sheldon RD, Albano E, Ellis AE, Hawk MA, Murphy S, Duong L, Rahmy S, Lu X, Jones RG and Schafer ZT. Acod1 expression in cancer cells promotes immune evasion through the generation of inhibitory peptides. Cell Rep 2024; 43: 113984.

[61] Zeng YR, Song JB, Wang D, Huang ZX, Zhang C, Sun YP, Shu G, Xiong Y, Guan KL, Ye D and Wang P. The immunometabolite itaconate stimulates OXGR1 to promote mucociliary clearance during the pulmonary innate immune response. J Clin Invest 2023; 133: e160463.

[62] Azizi SA, Qiu T, Brookes NE and Dickinson BC. Regulation of ERK2 activity by dynamic S-acylation. Cell Rep 2023; 42: 113135.

[63] Song KH, Kim SH, Noh KH, Bae HC, Kim JH, Lee HJ, Song J, Kang TH, Kim DW, Oh SJ, Jeon JH and Kim TW. Apoptosis inhibitor 5 increases metastasis via erk-mediated MMP expression. BMB Rep 2015; 48: 330-335.
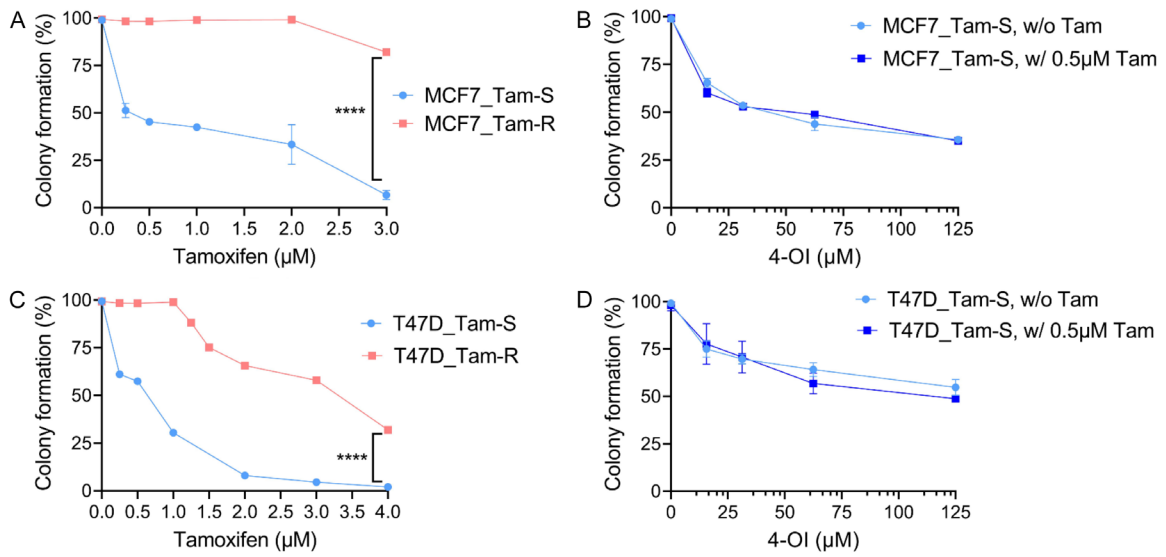
Supplementary Figure 1. Colony formation of various doses of (A) 4-OH-tamoxifen in MCF7 tamoxifen-sensitive (Tam-S) and tamoxifen-resistant (Tam-R) cells, (B) 4-OI in combination with 0.5 μM 4-OH-tamoxifen treated MCF7_Tam-S cells, (C) 4-OH-tamoxifen in T47D tamoxifen-sensitive (Tam-S) and tamoxifen-resistant (Tam-R) cells, and (D) 4-OI in combination with 0.5 μM 4-OH-tamoxifen treated T47D_Tam-S cells. An equal volume of the medium as control. Representative images and the data are shown as mean ± SEM from three experiments. ****P < 0.0001 among groups; two-way ANOVA.
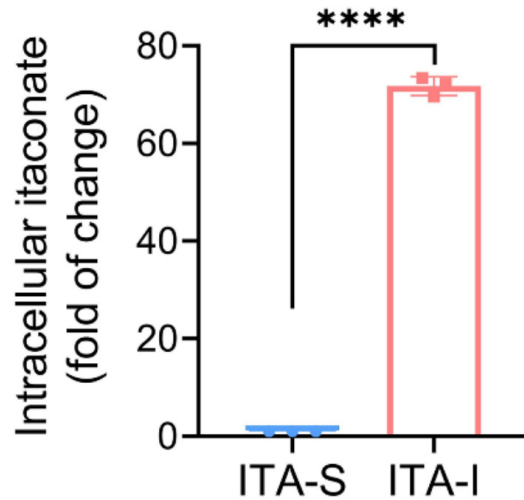
Supplementary Figure 2. Itaconate level (fold change) in itaconate-sensitive (ITA-S) and itaconate-insensitive (ITA-I) MCF7 cells.

Supplementary Figure 3. A. Analysis of phosphorylated TEY motif of ERK2 using Western blotting in MCF7 cells expressing Vector, ERK2_WT, ERK2_C254S, and ERK2_T185Q, following immunoprecipitation with the FLAG antibody. B. Densitometry analysis of Western blot results for phosphorylated TEY motif of ERK2 in MCF7 cells expressing Vector, ERK2_WT, ERK2_C254S, and ERK2_T185Q. C. Data from MCF7_Tam-S cells treated with 50 μM 4-OI alone or in combination with 0.5 μM 4-OH tamoxifen for 4 hours and MCF7_Tam-R cells for 16 hours. D. Data from T47D_Tam-S cells treated with 50 μM 4-OI alone or in combination with 0.5 μM 4-OH tamoxifen for 4 hours and T47D_Tam-R cells for 16 hours. E. Western blot analysis of phosphorylated TEY motif of ERK2 in MCF7_Tam-R cells expressing Vector, ERK2_T185E, and ERK2_T185A. The data are presented as mean ± SEM from three independent experiments. Statistical significance is indicated by *P < 0.05, **P < 0.01, ***P < 0.001, ****P < 0.0001 among groups; analyzed using two-way ANOVA.

Supplementary Figure 4. Quantification of API5 with Dapi was carried out using Pearson's correlation coefficient r. The minimal r value for significant colocalization is 0.5 (horizontal line). Data are presented as the mean ± SEM.